

# Performance Comparison of Geometric and $\mathcal{H}_\infty$ Fault Detection Filter Design: A Commercial Aircraft Example \*

Bálint Vanek \* Zoltán Szabó \* András Edelmayer \*  
József Bokor \*

\* Systems and Control Laboratory, Computer and Automation Research Institute, Hungarian Academy of Sciences (vanek@sztaki.hu).

**Abstract:** Geometric fault detection and isolation filters are known for having excellent fault isolation, fault reconstruction and sensitivity properties under small modeling uncertainty and noise. However they are assumed to be sensitive to model uncertainty and noise. This paper proposes a method to incorporate model uncertainty into the design. First, a geometric filter is designed on the nominal plant. Next a robust model matching problem is solved to design a post-filter that augments the performance of the geometric filter over the set of uncertain plants. The method is compared with the standard  $\mathcal{H}_\infty$  robust FDI filter design procedure, where the robustness and performance of the residual generation are solved in one step, but disturbance rejection and fault sensitivity are not decoupled from each other. Finally, an aircraft dynamics example is presented to detect and isolate aileron actuator faults to assess the performance of the different filter designs.

## 1. INTRODUCTION

Modern fly-by-wire aircraft flight control systems are becoming more complex with many actuators controlling several aerodynamic surfaces. While performance goals, like aerodynamic drag minimization and structural load alleviation are becoming more and more important flight must be kept at the same highest safety level. In parallel, there is a clear trend towards the All-Electric Aircraft. Recently, Airbus introduced on the A380 a new hydraulics layout (Van den Bossche, 2006), where the three Hydraulics circuitry is replaced by a two Hydraulics plus two Electric layout, which saves one ton mass for the aircraft. Each primary surface has a single hydraulically powered actuator and electrically powered back-up with the exception of the outer aileron, which uses the two hydraulic systems together. Consequently, the trends of complexity and more-electric architectures, like Electromechanical Actuators (EMA) with more fault sources, raise the importance of availability, reliability and operating safety. For safety critical systems, like aircraft, the consequences of faults in the control system hardware and software are deeply analyzed and rigorous design constraints are applied for ensuring compliance with stringent safety regulations of FAA, EASA and other aviation authorities. However, there is a growing need for on-line supervision and fault diagnosis to satisfy the newer societal imperatives towards an environmentally-friendlier aircraft with still the highest level of safety and reliability. The traditional approach to fault diagnosis in the wider application context is based on hardware redundancy methods which use multiple sensors, actuators computers and software to measure and control a particular variable (Goupil, 2011). Based on the mathematical model of the plant, analytical relation between different sensor outputs can be used to generate residual signals. There is a growing interest in methods which do not require additional hardware redundancy, and only rely on the ever increasing level of computational power onboard the aircraft. In analytical redundancy schemes,

the resulting difference generated from the consistency checking of different variables is called as a residual signal. The residual should be zero when the system is normal, and should diverge from zero when a fault occurs in the system. This zero and non-zero property of the residual is used to determine whether or not faults have occurred. Analytical redundancy makes use of a mathematical model and the goal is the determination of faults of a system from the comparison of available system measurements with a priori information represented by the mathematical model, through generation of residual quantities and their analysis. Various approaches have been applied to the residual generation problem, the parity space approach (Chow and Willsky, 1984), the multiple model method (Chang and Athans, 1978), detection filter design using geometric approach (Massoumnia, 1986), frequency domain concepts (Frank, 1990), unknown input observer concept (Chen and Patton, 1999), dynamic inversion based detection (Edelmayer et al., 2003), and using rational nullspace bases (Varga, 2003). Most of these design approaches refer to linear time-invariant (LTI) systems. The geometric concept is further generalized to linear parameter-varying (LPV) systems by Balas et al. (2003), while input affine nonlinear systems are considered by De Persis et al. (2001). The basic concepts underlying observer-based fault detection and isolation (FDI) schemes are the generation of residuals and the use of an optimal or adaptive threshold function to differentiate faults from disturbances, see the surveys of Frank (1990); Patton and Chen (1996). Generally, the residuals, also known as diagnostic signals, are generated by the FDI filter from the available input and output measurements of the monitored system. The threshold function is used to robustify the detection of the fault by minimizing the effects from false faults, disturbances and commands on the residuals. For fault isolation, the generated residual has to include enough information to differentiate said fault from another, usually this is accomplished through structured residuals or directional vectors. Robustness of the FDI algorithm is determined by its capability to decouple the filter performance outputs from disturbances, errors, and unmodelled dynamics. The rise of robust control techniques in the 1980s led to an interest in alternatives to the well known Kalman filter (Kalman, 1960), e.g. the  $\mathcal{H}_2$  filter (a generalization of the Kalman

\* This work is supported by the ADDSAFE (Advanced Fault Diagnosis for Sustainable Flight Guidance and Control) EU FP7 project, Grant Agreement: 233815, Coordinator: Dr. Andrés Marcos and in part by the BONUS HU 08 - ADD SAFE program of the Hungarian National Development Agency. This work is also supported by the Control Engineering Research Group of HAS at Budapest University of Technology and Economics.

filter) and the  $\mathcal{H}_\infty$  filter ((Shaked and Theodor, 1991)). These methods assume the signals are generated by a known dynamic model and robustness with respect to model uncertainty is an important consideration. Numerous papers on robust filter design have appeared (Appleby et al., 1991; Mangoubi, 1995; Sun and Packard, 2003; Scherer and Köse, 2008).

The importance of this paper is on the application (simulation) of the geometric approach based LTI FDI technique to a nonlinear high-fidelity aircraft model, where issues of model uncertainty, realistic disturbances and robustness have to be accounted for in the design stage. This paper proposes a method which incorporates model uncertainty into the design. First, a geometric filter is designed on the nominal plant. Next a robust model matching problem is solved to design a filter that robustly matches the performance of the geometric filter over the set of uncertain plants which is compared with the conventional one-step  $\mathcal{H}_\infty$  formulation of the problem. The remainder of the paper is structured as follows. Section 2 presents the basic concepts of geometric fault detection filter design. Section 3 formulates the robust fault detection filter design problem and describes the proposed solution method. The application example of a civil aircraft is described in Section 4. The method is applied to the high-fidelity aircraft model example, which demonstrates the proposed approach, given in Section 5. Finally, the paper is concluded in Section 6.

## 2. GEOMETRIC FDI FILTERS

The geometric design approach (Massoumnia, 1986) is known for its excellent fault isolation, fault reconstruction and sensitivity properties under small modeling uncertainty and noise. It is shown in (Seiler et al., 2011a) the robust model matching problem has an interesting self-optimality property for multiplicative input uncertainty sets. Specifically, the filter designed on the nominal plant is the optimal filter in the robust model matching problem. The derivation of the geometric FDI filters is presented for LTI systems with no disturbance, no uncertainty and the detection and isolation of two faults. Consider the LTI system with two additive actuator faults:

$$\begin{aligned}\dot{x}(t) &= Ax(t) + Bu(t) + L_1f_1(t) + L_2f_2(t) \\ y(t) &= Cx(t)\end{aligned}\quad (1)$$

where  $L_1$  and  $L_2$  represent the faults directions in the state space.  $f_1$  and  $f_2$  are the fault signals. The fault signals are zero if there is no fault but nonzero if the particular fault occurs. Only actuator faults are considered here but sensor faults can also be considered within the theory. The fundamental problem of residual generation is to synthesize residual generators (filters) with outputs  $r_i$  ( $i = 1, 2$ ) that have the following decoupling property:  $r_i$  is sensitive to  $f_i$  but insensitive to  $f_j$ ,  $i \neq j$ . More precisely, if  $f_i = 0$  then  $\lim_{t \rightarrow \infty} r_i(t) = 0$  and if  $f_i \neq 0$  then  $r_i \neq 0$ .

The solution of this problem depends on the  $(C, A)$ -invariant subspaces and certain unobservability subspaces (Massoumnia, 1986). A  $(C, A)$ -unobservability subspace  $\mathcal{S}$  is a subspace such that there exist matrices  $G$  and  $H$  with the property that  $\mathcal{S}$  is the maximal  $(A + GC)$  invariant subspace contained in  $\text{Ker } HC$ . The family of  $(C, A)$ -unobservability subspaces containing a given set  $\mathcal{L}$  has a minimal element. Define  $\mathcal{L}_i = \text{Im } L_i$  ( $i = 1, 2$ ) and denote by  $\mathcal{S}^*$  the smallest unobservability subspace containing  $\mathcal{L}_2$ . Then the fundamental problem of residual generation has a solution if and only if  $\mathcal{S}^* \cap \mathcal{L}_1 = 0$  (Massoumnia et al., 1989). The condition  $\mathcal{S}^* \cap \mathcal{L}_1 = 0$  ensures that the fault to be detected is not hidden in the unobservability subspace of the detection filter. In fact, the fault direction will be decoupled from the rest of the fault directions since

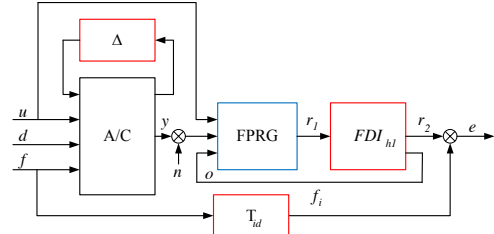


Fig. 1. Geometric FPRG filter with  $\mathcal{H}_\infty$  augmentation.

they are contained in the unobservability subspace of the residual generator. This result can be extended to LPV systems (Balas et al., 2003) and to nonlinear input affine systems (De Persis et al., 2001).

The residual generator associated with fault direction  $L_1$  can be described by an observer of the form:

$$\dot{w}(t) = Nw(t) - Gy(t) + Fu(t) \quad (2)$$

$$r_1(t) = Mw(t) - Hy(t)$$

where  $u$  and  $y$  are the known input and measured output signals of the original LTI system.  $w$  is the state of the residual generator and  $r_1$  is the residual.

Denote by  $P$  the projection operator  $P : \mathcal{X} \rightarrow \mathcal{X}/\mathcal{S}^*$ . The state matrices can be determined as follows (Massoumnia, 1986).  $H$  is a solution of the equation  $\text{Ker } HC = \text{Ker } C + \mathcal{S}^*$ , and  $M$  is the unique solution of  $MP = HC$ . Consider a gain matrix  $\hat{G}$  chosen such that  $(A + \hat{G}C)\mathcal{S}^* \subseteq \mathcal{S}^*$  and define  $\hat{A} = P(A + GC)P^T$ .  $\hat{A}$  is not necessarily Hurwitz. To obtain quadratically stable filters one can set  $N = \hat{A} + \tilde{G}M$ , where  $\tilde{G} := X^{-1}K$  and  $X, K$  are determined from the linear matrix inequality (LMI):

$$0 \succeq \hat{A}^T X + X \hat{A} + M^T K^T + KM \quad (3)$$

$$0 \preceq X = X^T \quad (4)$$

Then set  $G = P\hat{G} + \tilde{G}H$  and  $F = PB$ .

Using this approach there are as many filters as faults to detect, and their state dimensions are equal to the dimension of  $\mathcal{X}/\mathcal{S}^*$ . The filter poles can be tuned by imposing constraints in the LMI resulting in perfect reconstruction of fault signals  $f_i$ . One issue is that the filter design does not consider model uncertainty and the fault detection performance may be not be robust. The next section discusses a model matching approach for recovering the geometric filter performance in the presence of model uncertainty.

## 3. ROBUST MODEL MATCHING AUGMENTATION

It is a standard procedure to pose the FDI filter design problem as an  $\mathcal{H}_\infty$  optimization (Marcos et al., 2005). In this approach fault reconstruction is achieved as a model matching problem as shown in Fig. 2 and approximate disturbance decoupling is achieved in the  $\mathcal{H}_\infty$  optimal sense.

On the other hand the FPRG approach is able to provide exact decoupling between the fault(s) and the disturbances, but the resulting FPRG filter dynamics might not be optimal for the detection purpose. To overcome this weakness of the geometric approach, the FPRG filter can be augmented with a post-filter, as shown in Fig. 1, where the dynamics of the FPRG filter is shaped with suitable output injection  $o$ . Fault reconstruction is achieved with model matching using the  $\mathcal{H}_\infty$  optimal filter  $FDI_{hi}$ , which uses the independent outputs of the FPRG filter  $r_1$ . The main advantage of this approach is that elements of  $r_1$  are

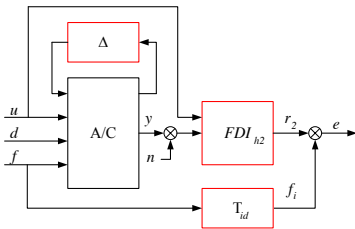


Fig. 2. Standard  $\mathcal{H}_\infty$  FDI filter architecture.

all decoupled from the disturbances and hence the filter  $FDI_{h1}$  only acts on the signals which are sensitive for the faults and can be fed back to shape the dynamics of the FPRG filter.

#### 4. AIRCRAFT MODEL

##### 4.1 General Aircraft Characteristics

The aircraft model used in this paper is an aircraft from Airbus. The aircraft has two engines and a nominal weight of 200 tons. Some of its performance at cruise flight condition are speed of 240 knots, altitude of 30000 ft. The aircraft has 19 control inputs, and measurement of 6-DOF motion with load factor ( $n_x, n_y, n_z$ ), body rate ( $p, q, r$ ), velocity ( $V_T$ ), aerodynamic angles ( $\alpha, \beta$ ), position ( $X, Y, Z$ ) and attitude ( $\phi, \theta, \psi$ ) outputs. The inputs are:  $pi$  left and  $pi$  right engine;  $AF$  (airbrake), which is disabled at cruise flight condition,  $\delta_{a,IL}$  Aileron internal Left;  $\delta_{a,IR}$  Aileron internal Right;  $\delta_{a,EL}$  Ail external Left;  $\delta_{a,ER}$  Ail external Right;  $\delta_{sp,1L}$  Spoiler 1 Left;  $\delta_{sp,1R}$  Spoiler 1R; Spoiler 23L; Spoiler 23R; Spoiler 45L; Spoiler 45R;  $\delta_{sp,6L}$  Spoiler 6L;  $\delta_{sp,6R}$  Spoiler 6R;  $\delta_{e,L}$  Elevator Left;  $\delta_{e,R}$  Elevator Right;  $\delta_r$  Rudder; and  $\delta_{ih}$  Trimmable Horizontal Stabilizer which is used for trimming purposes.

The aerodynamic database, propriety of Airbus Operations S.A.S, is of high-fidelity. The rigid body aircraft equations of motion are augmented with actuator (Goupil, 2011) and sensor characteristics. The nonlinear body-axes rigid body dynamics includes 12 states:  $p, q, r$  body rates,  $u, v, w$  velocities all in body axes,  $\phi, \theta, \psi$  Euler angles, representing the rotation between the body and inertial axes, and  $X, Y, Z$  positions in the North-East-Down coordinate frame, assuming Flat Earth for simplicity. The rigid body aircraft model is augmented with nonlinear actuator and sensor models on all input and output channels.

##### 4.2 Linearized Aircraft Model

In the present article one design point, cruise flight condition, is considered. The LTI model of the aircraft is obtained at level flight, with  $p = q = r = 0$  rad/s,  $v_x = const.$  m/s,  $v_y = 0$  m/s,  $v_z = const.$  m/s, at 9144 m altitude, see Vanek et al. (2011) for details. The airbrake, which is disabled at high Mach numbers, is removed from the control inputs since it has no effect on the aircraft. The model used for trim is an open-loop model without the control loop and, since the actuators and sensors are assumed to have unit steady state gain and low-pass characteristics, their dynamics are omitted. Trim is obtained with zero aileron, rudder and elevator deflection, left and right engines are providing the same amount of thrust to balance the yawing motion. Pitch axis trim is obtained with the Trimmable Horizontal Stabilizer, while the aircraft has constant angle-of-attack. The resulting 12 state linear model is unstable.

The open loop aircraft model is slightly unstable around the yaw angle ( $\psi$ ), and has two modes ( $X, Y$ ) which are integrators. Since the FDI problem is invariant of

$X, Y$  positions and yaw angle these states are removed from the dynamics. The resulting model with nine states, as described in (Vanek et al., 2011), almost perfectly matches the original 12 states model in the behavior of the remaining states, and outputs. The resulting system with nine states is stable which is necessary for linear estimator based FDI techniques. After investigation of the FCC commands, assuming faults appear only on the aileron, elevator, and rudder channels, the inputs of the system can be simplified. The two engines are receiving the same commands, the spoilers have a fixed coupling, the two elevators are also moving in unison, hence the number of inputs can be reduced to 9, namely:  $pi$  engine;  $\delta_{a,IL}$  Aileron internal Left;  $\delta_{a,IR}$  Aileron internal Right;  $\delta_{a,EL}$  Ail external Left;  $\delta_{a,ER}$  Ail external Right;  $\delta_{sp}$  Spoiler  $\delta_e$  Elevator;  $\delta_r$  Rudder; and  $\delta_{ih}$  trimmable horizontal stabilizer. The resulting LTI model is augmented with first order sensor and actuator dynamics derived from the high-fidelity simulation, to account for their effect on the aircraft behavior.

#### 5. FDI FILTER DESIGN FOR THE AIRCRAFT

A geometric LTI FDI filter is designed for the left inner aileron fault detection problem of the aircraft. First, the filter design steps are detailed and supported by linear analysis plots to show the optimality of the geometric filter. Detailed simulations on the high-fidelity aircraft model with injected aileron faults follows.

##### 5.1 Filter Design Steps

The main idea behind the filter design formulation is that aileron faults appear on the filter residual output, while elevator and rudder faults are embedded in the unobservability subspace of the filter. For that reason the LTI model derived in Section 4.2 is augmented with left inner aileron, left elevator, and rudder faults, by using the successive input directions from the  $B$  and  $D$  matrices as fault directions in the linear model. Load factor,  $n_x, n_y$ , and  $n_z$ , measurement is omitted from the model, since the  $D$  matrix associated with these acceleration outputs is nonzero, which makes the geometric FDI synthesis more complicated. The resulting design model has 9 outputs, 12 inputs (including the three fault directions) and 27 states, including actuator and sensor dynamics. While the obtained filter, using the methods developed in (Massoumnia, 1986), has 7 residual outputs, 18 inputs, and 18 states. Since perfect decoupling is possible, the transfer functions between elevator to residual and rudder to residual are zero, while the residual all have nonzero response for aileron faults. To be able to augment the FPRG filter with an  $\mathcal{H}_\infty$  post filter using output injection the original 18 inputs of the system are augmented by 18 additional inputs, each of them directly acting on one of the 18 states of the original FPRG filter. To pose an  $\mathcal{H}_\infty$  optimization problem for the post filter, a suitable weighted interconnection have to be developed as shown in Figure 3. The list of design weight are the following:  $W_u$  represents the uncertainty weights,  $W_{dr}$  is responsible for Dryden wind gust disturbance, sensor noise is filtered through  $W_d$ , while fault tracking error is penalized by  $W_e$  and to for well posedness the pseudo control signals of the  $\mathcal{H}_\infty$  filter are penalized by  $W_p$ . Fault tracking is achieved only in a limited frequency range described by  $T_{id}$ , the weighted interconnection with the FPRG filter including has 29 states, 26 outputs and 43 inputs, and the resulting  $\mathcal{H}_\infty$  FDI filter, not considering the effects of uncertainty  $\Delta$ , has 7 measurements and 19 control outputs. Combining the FPRG filter and the FDI filter results in a 30 states, 18 input and 1 output filter after model order reduction. On the other hand if we solve for the FDI filter in one step without including the FPRG filter, than  $W_p$  can be omitted, but still the weighted interconnection has 31 states (2 more than the previous case), 28 outputs and 25

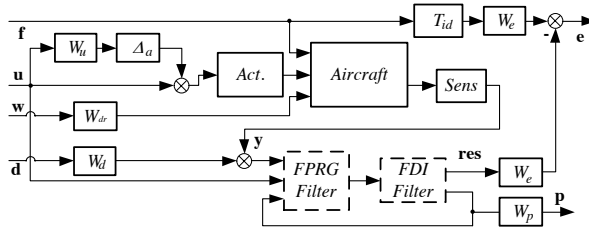


Fig. 3. Input multiplicative uncertainty case, Weighted interconnection for  $\mathcal{H}_\infty$  filter synthesis.

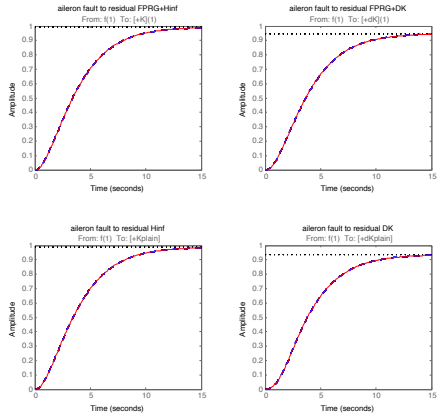


Fig. 4. Input multiplicative uncertainty case, fault to residual response.

inputs, while the resulting FDI filter, solving the complete problem has 29 states, 1 output and 18 inputs. While both of them achieves a  $\gamma$  value of 0.0016, indicating that without uncertainty the FDI problem is feasible and the resulting solutions are almost the same. Moreover, if we include input multiplicative uncertainty in the design (0.01 in low frequency and 0.2 in higher frequencies) with  $W_u$  and  $\Delta$ , and obtain the FDI filters with DK iteration, the resulting filters will still have similar characteristics, as projected by (Seiler et al., 2011b).

On the other hand, if we use output multiplicative uncertainty on the sensor measurements with similar design weights of 0.01 uncertainty in low and 0.2 uncertainty at high frequencies, the resulting  $\mathcal{H}_\infty$  and  $\mu$  optimal filters will differ significantly. The FPRG+ $\mathcal{H}_\infty$  solution achieves a worst case gain of 9.25, while the FPRG+ $\mu$  filter has 1.2106 value, indicating better handling of uncertainty. To put the figures in context the plain  $\mathcal{H}_\infty$  and  $\mu$  solution achieves worst case gain of 9.167 and 1.1213 respectively, which is only slightly lower than the combined FPRG solution.

To have more insight in the designs, the four filters are compared in linear simulation first. Figure 4 shows the residual output of the filters, including the nominal behavior (red) and the response of 40 randomly sampled models from the uncertainty space  $\Delta$  for a step change in aileron fault input. Excellent responses can be seen without any variation across the uncertain models which is due to the fact that input uncertainty does not change the geometrical properties of the plant and the decoupling is still valid after the uncertainty acts. All figures are normalized due to Airbus confidentiality reasons.

Figure 5 shows the singular values plot of the control inputs effect across the uncertain plants on the residual of the four filters. Notice that all of them achieves at least 20 dB attenuation on all control inputs combined, and even more attenuation is achieved on the disturbances to the residual channels.

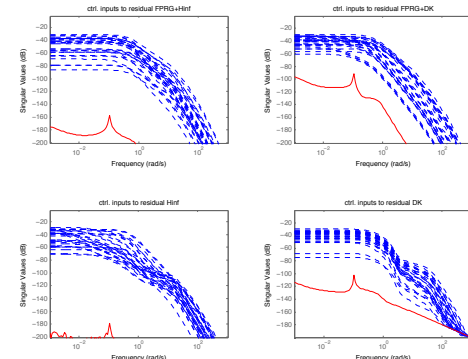


Fig. 5. Input multiplicative uncertainty case, effect of control inputs on residual.

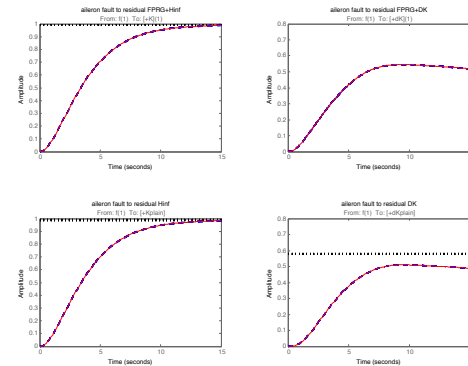


Fig. 6. Output multiplicative uncertainty case, fault to residual response.

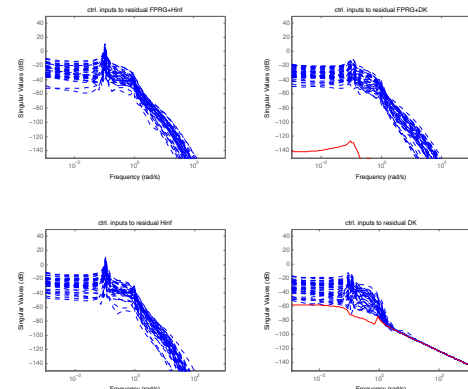


Fig. 7. Output multiplicative uncertainty case, effect of control inputs on residual.

If we analyze the effect of output uncertainty with similar level of model mismatch, shown in Fig. 6, the results are less ideal. The set of uncertain plants with the filters designed for the nominal plant (using  $\mathcal{H}_\infty$  synthesis), have the same fault tracking response, while the two designs taking uncertainty into consideration achieves less satisfactory fault tracking behavior, but the responses due to modeling error are not spread out. The difference between the designs can be seen on the control inputs to residuals plot (Fig. 7), where at least 20 dB difference can be seen between the  $\mathcal{H}_\infty$  and  $\mu$  designs, irrespective of if the FPRG pre-filter is applied to the plant or not. The peak of the sigma plot on the  $\mathcal{H}_\infty + FPRG$ ,  $\mu + FPRG$ ,  $\mathcal{H}_\infty$ , and  $\mu$  are 12dB, -11.3dB, 10.7dB, -12dB respectively, indicating slight edge over the plain one-step design.

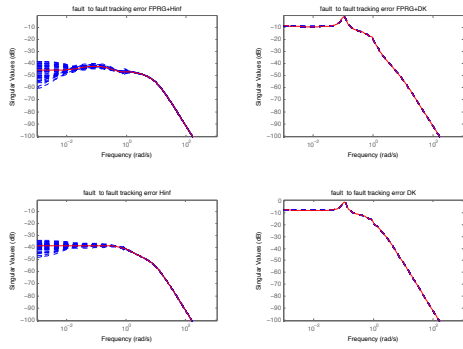


Fig. 8. Output multiplicative uncertainty case, fault to fault tracking error channel.

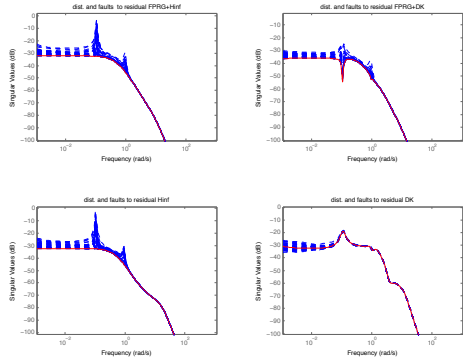


Fig. 9. Output multiplicative uncertainty case, effect of disturbances and additional control surface faults on residual.

The fault to fault tracking error singular value plot is shown in Figure 8. It is clear that both methods achieve better results, when the uncertainty is not taken into account during the design, and the results are very similar.

The effect of windgust disturbances and elevator or rudder faults to residual singular value plot is shown in Figure 9. Where the uncertainty plays an important role again. The peak of the sigma plot on the  $\mathcal{H}_\infty + FPRG$ ,  $\mu + FPRG$ ,  $\mathcal{H}_\infty$ , and  $\mu$  are  $-1.39dB$ ,  $-24.5dB$ ,  $-2.77dB$ ,  $-18.5dB$  respectively, indicating a slight advantage of the FPRG based design.

To further analyze the performance of the filters, the  $\mathcal{H}_\infty + FPRG$  and the  $\mathcal{H}_\infty$  based solution are applied to the nonlinear aircraft model after taking the trim values into consideration, on both control input and sensor output signals. Since the simulation is implemented under SIMULINK with 0.01sec fixed step size, the corresponding filters are also discretized with the same sampling time using bilinear transformation, the investigation with the  $\mu$  based filters are omitted since their high frequency poles prohibited their implementation with 0.01sec sampling time. It is also worth mentioning, that the simulation is in closed-loop with the flight control system set to altitude and heading hold mode and moderate atmospheric windgust disturbances are perturbing the aircraft flight. For threshold selection purposes the filters are applied to the nonlinear aircraft model at various cruise conditions with appropriate trim scheduling, moderate Dryden windgust disturbance. The Left elevator drifts from commanded position with 5 deg/s rate starting at 20 s. The simulation starts from a typical flight condition of 200knots and 26000ft, c.g. position is  $x_{cg} = 0.3$  and weight is 200000kg. The change in aircraft behavior is clearly noticeable, large pitch excursion can be seen on Figure 10, while the flight control system counteracts with the adjacent elevator. Both LTI FDI residual have very similar behavior as they reach maximum 0.175 value. The main advantage of the FPRG design lies

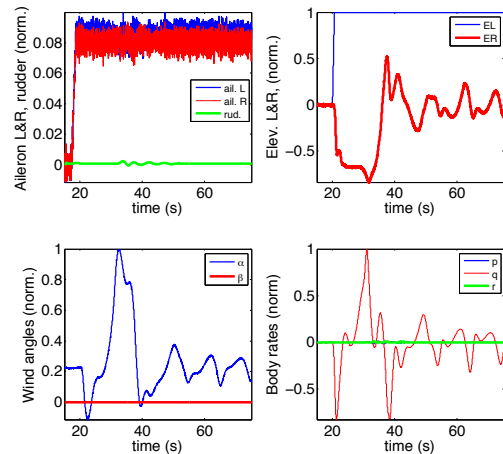


Fig. 10. Left elevator runaway scenario, fault occurs at 20s.

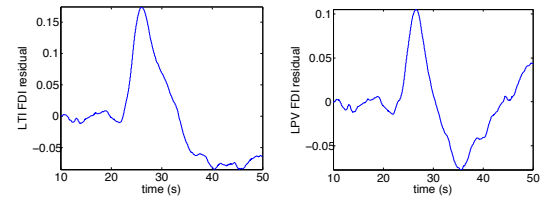


Fig. 11. Left elevator runaway, LTI (left) and LPV (right) FDI filter residual.

in the fact, that it can be easily generalized to the linear parameter varying (LPV) case, where the aircraft model state space matrices are affine functions of velocity and altitude. The same algebraic solution can be obtained with the LPV description of the plant (Szaszi et al., 2005), without computationally expensive LMI optimization and the previously derived  $\mathcal{H}_\infty$  post filter can be applied to the LPV FPRG filter. The LPV FDI residual reaches only 0.105 value during the maneuver, indicating better fault isolation properties, hence detection thresholds are selected as  $0.105 \times 1.5$  and  $0.175 \times 1.5$  respectively.

The detection performance is analyzed on a left inboard aileron jamming scenario at 20s (bias on the rod sensor, shifts the surface with a normalized value of  $-0.134$  from commanded position). The flight is at a representative cruise condition, with moderate Dryden windgust, and off from the previously selected nominal design condition,  $V_{CAS} = 170knots$  and  $h = 23000ft$ ,  $x_{cg} = 0.3$ , and  $m = 200000kg$ .

Detection time performance (relative to the performance specification) of 0.00725 is achieved with the LTI approach and 0.00508 with the LPV method, LPV reconstruction performance is still excellent showing the advantage of the LPV method. Since the FPRG based solution is more suitable to design the filters with the LPV model it is more advantageous to use in FDI problems.

## 6. CONCLUSIONS

This paper considers the design of geometric fault detection filters and their application to a high fidelity aircraft model, and shows the advantages of advanced model-based methods, those are candidates for future industrial implementation. First, a geometric filter is designed on the nominal plant. Next a robust model matching problem is solved to design a filter that robustly matches the performance of the geometric filter over the set of uncertain plants. It is then shown that the robust model matching problem has an interesting self-optimality property for

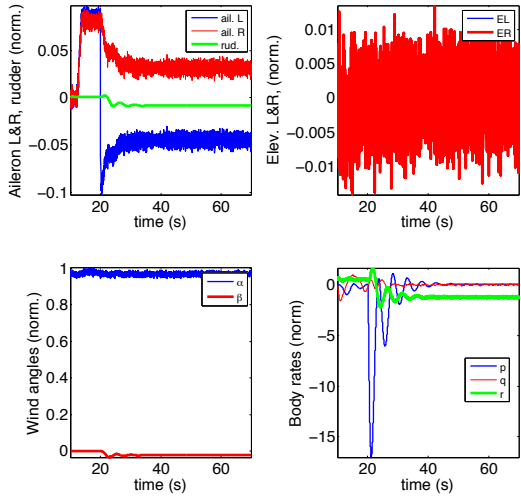


Fig. 12. Left aileron liquid jamming scenario, fault occurs at 20s.

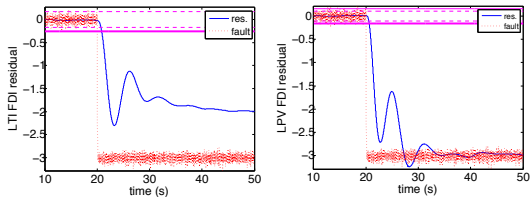


Fig. 13. Aileron liquid jamming, LTI (left) and LPV (right) FDI filter residual.

multiplicative input uncertainty sets. The proposed LTI filter is then applied to a high-fidelity aircraft model, where different aileron faults are successfully detected and when designed properly isolated from elevator and rudder faults in reasonable time. Further research should extend the validity of the present approach and based on the present findings provide a fault detection approach for a larger flight envelope.

## REFERENCES

- Appleby, B., Dowdle, J., and VanderVelde, W. (1991). Robust estimator design using  $\mu$  synthesis. In *Proc. of the IEEE Conference on Decision and Control*, 640–645.
- Balas, G., Bokor, J., and Szabo, Z. (2003). Invariant subspaces for LPV systems and their applications. *IEEE Transactions on Automatic Control*, 48(11), 2065–2069.
- Chang, C.B. and Athans, M. (1978). State estimation for discrete systems with switching parameters. *IEEE Transactions on Aerospace and Electronic Systems*, 14, 418–425.
- Chen, J. and Patton, R.J. (1999). *Robust Model-based Fault Diagnosis for Dynamic Systems*. Kluwer Academic, Boston.
- Chow, E. and Willsky, A. (1984). Analytical redundancy and the design of robust failure detection systems. *IEEE Trans. on Automatic Control*, 29(7), 603–614.
- De Persis, C., De Santis, R., and Isidori, A. (2001). Nonlinear actuator fault detection and isolation for a VTOL aircraft. In *Proceedings of the 2001 American Control Conference, Vols 1-6*, 4449–4454.
- Edelmayer, A., Bokor, J., and Szabo, Z. (2003). A geometric view on inversion-based detection filter design in nonlinear systems. In *Proceedings of the 5th IFAC symposium on fault detection, supervision and safety of technical processes. SAFEPROCESS 2003, Washington*, 783–788. Washington.
- Frank, P. (1990). Fault diagnosis in dynamic systems using analytical and knowledge-based redundancy - a survey and some new results. *Automatica*, 26, 459–474.
- Goupil, P. (2009). Airbus state of the art and practices on fdi and ftc. In *Proceedings of Safeprocess'09*.
- Goupil, P. (2011). Airbus state of the art and practices on fdi and ftc in flight control system. *Control Engineering Practice*, 19, 524–539.
- Kalman, R. (1960). A new approach to linear filtering and prediction problems. *Trans. ASME, Ser D., Journal of Basic Engineering*, 82, 35–45.
- Mangoubi, R. (1995). *Robust Estimation and Failure Detection For Linear Systems*. Ph.D. thesis, Massachusetts Institute of Technology.
- Marcos, A., S., G., and J., B.G. (2005). An application of  $H_\infty$  fault detection and isolation to a transport aircraft. *Control Engineering Practice*, 13(1), 105–119.
- Massoumnia, M. (1986). A geometric approach to the synthesys of failure detection filters. *IEEE Transactions on Automatic Control*, 31, 839–846.
- Massoumnia, M., Verghese, G., and Willsky, A. (1989). Failure detection and identification. *IEEE Transactions on Automatic Control*, 34, 316–321.
- Patton, R.J. and Chen, J. (1996). Robust fault detection and isolation FDI systems. *Contr. Dynamic Syst.*, 74, 176–224.
- Scherer, C. and Köse, I. (2008). Robustness with dynamic IQCs: An exact state-space characterization of nominal stability with applications to robust estimation. *Automatica*, 44, 1666–1675.
- Seiler, P., Bokor, J., Vanek, B., and Balas, G. (2011a). Robust model matching for geometric fault detection filters. In *American Control Conference (ACC), 2011*, 226–231.
- Seiler, P., Vanek, B., Bokor, J., and Balas, G. (2011b). Robust  $H_\infty$  filter design using frequency gridding. In *Submitted to the 2011 American Control Conference*.
- Shaked, U. and Theodor, Y. (1991).  $H_\infty$ -optimal estimation: A tutorial. In *Proc. of the IEEE Conference on Decision and Control*, 2278–2286.
- Sun, K. and Packard, A. (2003). Optimal, worst-case filter design via convex optimization. In *Proc. of the IEEE Conference on Decision and Control*, 1380–1385.
- Szaszi, I., Marcos, A., Balas, G., and Bokor, J. (2005). LPV detection filter design for a Boeing 747-100/200 aircraft. *AIAA Journal of Guidance, Dynamics and Control*, 28(3), 461–470.
- Van den Bossche, D. (2006). The a380 flight control electrohydrostatic actuators, achievements and lessons learnt. In *Proc. 25th Congress of the International Council of the Aeronautical Sciences*.
- Vanek, B., Seiler, P., Bokor, J., and Balas, G. (2011). Robust fault detection filter design for commercial aircraft. In *Euro GNC 2011 1st CEAS Specialist Conference on Guidance, Navigation & Control, München*.
- Varga, A. (2003). On computing least order fault detectors using rational nullspace bases. In *In Proceedings of the IFAC Symp. SAFEPROCESS'2003, Washington D.C.*